Trade-offs in Reliability and Performance Using Selective Beamforming for Ultra-Massive MIMO

Anis Hamadouche and Mathini Sellathurai

arXiv:2407.20135v2 [eess.SP] 25 Apr 2025

***Abstract*— This paper addresses the optimization challenges in Ultra-Massive MIMO communication systems, focusing on array selection and beamforming in dynamic and diverse operational contexts. We introduce a novel array selection criterion that incorporates antenna health information into the optimization process, distinguishing our approach from traditional methods. Our methodology employs dual proximal-gradient ascent to effectively tackle the constrained non-convex and non-smooth nature of sparse array selection problems. A central feature of our strategy is the implementation of proportional fairness among communication users, aligning with system resource limitations while ensuring minimum rate requirements for all users. This approach not only enhances system efficiency and responsiveness but also ensures equitable resource distribution. Extensive simulations validate the effectiveness of the proposed solutions in optimizing Ultra-Massive MIMO system performance, demonstrating their applicability in complex communication scenarios. Our findings reveal key trade-offs influenced by the sparsity promotion weight (γ). As γ increases, spectral efficiency (SE) and communication rate (Ri) decrease, while beamforming matrix density (BMD) reduces and antenna reliability (RL) significantly improves. These results highlight the critical balance between performance and reliability, essential for the practical deployment of Ultra-Massive MIMO systems. This work advances the field by providing innovative solutions and new insights into array selection and beamforming optimization, setting a foundation for future research in Ultra-Massive MIMO communication systems.**

***Index Terms*—Ultra-Massive MIMO (UM-MIMO); Beamforming; 5G; 6G; Optimisation Algorithms.**

I. INTRODUCTION

In today's cellular network landscape, the increasing demand for high-speed, reliable communication has led to a paradigm shift towards more dynamic and flexible system architectures. Modern cellular networks have evolved from static entities into vibrant ecosystems that must adapt in real-time to fluctuating user demands, varying network conditions, and stringent quality of service (QoS) requirements. This need for adaptability and responsiveness is particularly pronounced in Ultra-Massive MIMO communication systems, where the use of large antenna arrays presents unique challenges and opportunities [**hassanien2019dual**, **johnston2022mimo**, **hassanien2016non**, **cheng2021hybrid**, **boudaher2016towards**].

Adaptability in modern cellular networks is crucial for several reasons. First, user requirements are no longer uniform or predictable; they are diverse and dynamic [**networld202020145g**, **shafi20175g**, **chih20165g**, **akyildiz20165g**, **sun2015intelligent**]. Users expect seamless connectivity whether they are streaming high-definition videos, engaging in real-time gaming, or leveraging IoT devices for smart home applications. The network must adapt its resource allocation strategies in real-time to meet these varying demands without compromising speed, latency, or reliability [**sun2015intelligent**].

Secondly, the operational environment of cellular networks is inherently dynamic. Factors such as user mobility, interference from neighboring cells, and physical obstructions can dramatically alter network conditions. A responsive network can swiftly adjust its operational parameters, such as beamforming vectors [**liao2023robust**, **chen2022generalized**, **liu2022joint**, **cheng2022double**, **liu2020radar**, **yuan2020bayesian**], power levels [**9951144**, **9104262**, **9737562**, **8835674**, **9078732**], and frequency bands, to mitigate these effects and maintain optimal performance.

In Ultra-Massive MIMO systems, the need for adaptability and responsiveness is even greater. These systems operate in high-frequency mmWave bands, known for their vast bandwidth and high data rate potential, but also for their sensitivity to obstacles and rapid signal degradation over distance. The complexity of these systems requires them to manage communication needs while maintaining operational integrity for applications like target detection and tracking.

The introduction of fast algorithms in Ultra-Massive MIMO systems represents a significant step towards addressing these challenges. By adapting the beamforming weights while incorporating phased array elements' reliability information, these algorithms ensure that the system can respond in real-time to changes in user requirements, environmental conditions, and structural integrity. This results in a system that is not just reactive but proactive in maintaining service quality, operational efficiency, and system reliability.

Adaptability and responsiveness in modern cellular networks, especially in Ultra-Massive MIMO systems, are not just requirements; they are fundamental attributes that define operational efficacy and future readiness. As user demands and operational challenges continue to grow, the ability of these networks to dynamically adapt and respond will be crucial for their success and sustainability.

Proportional fairness, a longstanding principle in communication system design, aims to allocate resources such that increasing allocation to one user results in a proportionally larger decrease for another. This ensures each user receives a fair share of resources according to their needs.

In traditional scenarios, where users have uniform modulation schemes and QoS demands, proportional fairness is effective. It ensures an equitable distribution of resources and

Anis Hamadouche and Mathini Sellathurai are with the School of Engineering & Physical Sciences, Heriot-Watt University, Edinburgh EH14 4AS, UK (e-mail: {ah225,ah2161,m.sellathurai@}@hw.ac.uk).

a balanced user experience across the network.

However, modern communication networks are increasingly heterogeneous. Diverse services such as IoT devices, video streaming, online gaming, and real-time communications mean users now have different QoS needs. Additionally, advancements in communication technologies have introduced multiple modulation schemes, each with unique advantages and limitations. As a result, not all users are optimized for every modulation scheme.

In this context, traditional proportional fairness can lead to inefficiencies. For instance, allocating the same bandwidth to a high-definition video stream and a simple IoT sensor data transmission can waste resources. The video stream requires more bandwidth for smooth operation, while the IoT data will underutilize its allocation.

Utility proportional fairness emerges as a more appropriate solution in these complex environments. Here, "utility" represents a measure of user satisfaction or the effectiveness of resource allocation. Instead of equal resource shares, utility proportional fairness ensures each user derives an equal level of satisfaction or utility from their allocation. This translates to different resource amounts for different users, based on their QoS demands and modulation capabilities.

In conventional beamforming designs, power distribution across the antenna array typically overlooks the varying reliability or condition of individual antenna elements. This oversight can lead to scenarios where power is allocated to compromised or less reliable elements, resulting in suboptimal system performance and increased vulnerability to failures. By integrating a reliability matrix for phased array elements into the beamforming optimization process, the system can discern the reliability levels of individual elements and adjust its power distribution accordingly.

This integration leads to a sparse beamforming matrix, where power is concentrated on elements with higher reliability scores rather than being uniformly spread across the entire array. This approach ensures that the most dependable elements bear the transmission responsibility, significantly enhancing the system's resilience to element failures or degradation. In cases of structural damage or progressive wear and tear, this method allows the system to dynamically recalibrate its power distribution, continuously adapting to the evolving condition of the antenna array.

The advantages of this approach are manifold. It increases overall system reliability by bypassing or mitigating the impact of unreliable or damaged elements. It also enhances fault tolerance, ensuring the system maintains operational integrity and performance standards even when certain elements are compromised. This resilience is crucial in scenarios where uninterrupted operation is paramount, such as in critical communication infrastructure or defense applications.

Moreover, incorporating structural sparsity knowledge into beamforming design fosters the development of more intelligent and adaptive Ultra-Massive MIMO communication systems. By enabling the system to self-assess and dynamically adjust to its structural health, this approach introduces self-awareness and self-optimization, significant strides towards smarter, more autonomous communication systems.

Our contributions to Ultra-Massive MIMO communication systems are characterized by:

- The introduction of a new array selection criterion that integrates antenna health information for beam pattern correction and enhanced system reliability;
- The use of lightweight optimization techniques like gradient dual ascent and proximal-gradient dual ascent to directly tackle nonconvex challenges in sparse array selection without unnecessary mathematical relaxation;
- Ensuring proportional fairness among communication users, aligning with resource constraints and guaranteeing minimum rate requirements. This comprehensive approach not only enhances system efficiency and responsiveness but also ensures equitable resource distribution, making it highly relevant for modern communication systems.

This paper is organized into six main sections for a comprehensive exploration of the research topic. Section II, "Related Work," reviews pertinent literature, contextualizing our study within the broader scope of existing research in Ultra-Massive MIMO communication systems. Section III, "Problem Formulation," presents the joint communication beamforming problem as an optimization problem, introducing the mathematical system models and setting the stage for the discussion of our proposed methodologies. Section IV, "Antenna-Health Aware Beamforming," introduces the Proximal Gradient Dual Ascent (PGDA) algorithm, emphasizing its adaptiveness and efficiency in managing spectral resources and maintaining system reliability. Section V, "Experimental Results," rigorously evaluates our proposed solutions, substantiating our theoretical claims with empirical data and insightful analysis. Finally, Section VI, "Conclusion," encapsulates the key findings, discusses the implications of our research, and offers a perspective on potential future directions in Ultra-Massive MIMO communication systems.

II. RELATED WORK

Compared to traditional methods, our approach offers a more comprehensive and adaptive solution for beamforming and array selection in Ultra-Massive MIMO communication systems. Techniques commonly used by researchers such as Xu et al. (2023) [**10190916**] and Wu et al. (2022) [**9777612**] often rely on semidefinite relaxation (SDR) and alternating optimization. While these methods are effective, they may not fully account for the dynamic nature of Ultra-Massive MIMO environments and can be computationally intensive.

Our method, on the other hand, introduces a novel array selection criterion that incorporates prior information about the system's health directly into the optimization problem. By using gradient dual ascent and dual proximal-gradient ascent for sparse array selection, we address the nonconvex challenges inherent in these systems more directly. This approach excels in faster convergence and better adaptability to changing conditions, making it ideal for real-time applications in dynamic environments.

Additionally, our solution strikes an optimal balance between various communication objectives, ensuring proportional fairness among users. This is particularly important in

scenarios with stringent resource constraints, where equitable distribution is critical. By guaranteeing a minimum rate requirement for each user, our approach not only maximizes overall system performance but also ensures fairness and efficiency across the network.

III. Problem Formulation

Consider a millimeter wave (mmWave) communication node equipped with N_t transmit antennas and N_r receive antennas. This node services M users, each having a single antenna. Assume $\mathbf{X}$ represents a narrow-band transmit matrix of dimensions $N_t \times L$, expressed as:

$$\mathbf{X} = \mathbf{W}\mathbf{S} \tag{1}$$

where $L > N_t$ is the duration of the signal frames, $\mathbf{W} = [\mathbf{w}_1, \cdots, \mathbf{w}_M]^T$ is the beamforming matrix that needs designing with $\mathbf{w}_j$ being the j-th beamforming vector, and $\mathbf{S} \in \mathbb{C}^{M\times L}$ represents the data stream.

We assume that these data streams are independent, hence

$$\frac{1}{L}\mathbf{S}\mathbf{S}^H = \mathbf{I}_{N_t} \tag{2}$$

This equation holds asymptotically when the signaling adopts a Gaussian distribution and L is sufficiently large.

Equation (2) demonstrates that the data streams remain orthogonal throughout the frame's duration L, ensuring no interference occurs among them. This orthogonality is a common stipulation in numerous communication systems to prevent interference across different data streams. The term on the right, $\mathbf{I}_{N_t}$, denotes the identity matrix for size N_t, indicating that when the data streams are cross-multiplied with their Hermitian transposes ($\mathbf{S}^H$), they yield an identity matrix, scaled by the length of the frame L.

The received communication signal $\mathbf{Y}^c \in \mathbb{C}^{M\times L}$ is described by:

$$\mathbf{Y}^c = \mathbf{H}^H\mathbf{X} + \mathbf{N}, \tag{3}$$

where $\mathbf{N} \in \mathbb{C}^{M\times L}$ represents the additive white Gaussian noise (AWGN) matrix, each element possessing a variance σ_c^2. Furthermore, $\mathbf{H} = [\mathbf{h}_1, \cdots, \mathbf{h}_M] \in \mathbb{C}^{N_t\times M}$ denotes the communication channel matrix, with $\mathbf{h}_j \in \mathbb{C}^{N_t}$ indicating the channel corresponding to the j-th user. The signal-to-interference-plus-noise ratio (SINR) for the m-th user is then calculated as:

$$\gamma_m = \frac{|\mathbf{h}_m^H\mathbf{w}_m|^2}{\sum_{j\neq m}|\mathbf{h}_m^H\mathbf{w}_j|^2 + \sigma_c^2}, \tag{4}$$

in which the term $\sum_{j\neq m}|\mathbf{h}_m^H\mathbf{w}_j|^2$ quantifies the interference from other users affecting the m-th user.

A. Antenna-Health constraints

In a phased array system equipped with N antenna elements and M RF chains, the interactions between these components—mediated through beamforming weights that adjust phase and amplitude—are encapsulated by a matrix β with dimensions $N \times M$. This matrix represents the health and operational status of each antenna element in relation to the RF chains. Each element, $\beta_{i,j}$, within the matrix indicates the reliability or operational health of the connection between the i-th RF chain and the j-th antenna element, with values ranging from 0 (denoting complete failure or an off state) to 1 (indicating full operational status). This reliability measure can encompass the operational integrity of individual components such as power amplifiers, attenuators, phase shifters, or directly reflect the antenna elements' reliability. In cases where only the antenna elements are considered, β reduces to a vector of length N, where each β_i', for $i = 1, \ldots, N$, quantifies the reliability of the i-th antenna element. Here, N represents the total number of antenna elements, denoted as N_t for transmitters and N_r for receivers.

Assessing system reliability involves a multifaceted process that includes simulations, far-field and near-field measurements, network analysis, and environmental testing. These measures are designed to identify and mitigate potential performance degradations. Continuous monitoring and advanced correction algorithms are crucial to maintain the efficiency and reliability of phased array systems.

The following section will discuss strategies to jointly select the most reliable antenna elements subject to the minimum quality of service (QoS) of communication users while considering power limitations.

IV. Antenna-Health Aware beamforming

In practical applications, incorporating the reliability data of phased array elements into the beamforming optimization problem marks a significant evolution towards more robust, dependable, and fault-tolerant UM-MIMO systems. This method optimizes resource utilization by directing power towards the most reliable elements, thereby guaranteeing continuous and efficient operation even amidst structural challenges. Such an approach not only enhances system resilience but also establishes a new benchmark in the design and functioning of sophisticated communication systems.

Prior information about the phased array structural/connection reliability can be embedded as a structured sparsity into the optimisation problem as follows:

$$\max_{\mathbf{w}_j,\forall j} \quad \sum_{j=1}^{M}\rho_j\log(1+\gamma_j) - \rho_s\sum_{i,j}(1-\beta_{i,j})|w_{i,j}| \tag{5a}$$

$$\text{s.t.} \quad \text{trace}(\mathbf{w}\mathbf{w}^H) \leq P_t, \tag{5b}$$

$$R_{\min_j} \leq \log\left(1+\gamma_j\right), \forall m. \tag{5c}$$

where we multiply each beamforming element by a corresponding failure mask $\beta_{i,j}$ capturing the reliability of the i-th antenna element to j-th RF chain connection. ρ_s is a regularisation parameter that promotes sparsity and ρ_j are the communication bandwidth allocation proportion weights.

Adding the sparsity promoting step yields a nonsmooth nonconvex optimisation problem that can be solved using Algorithm 1, where

$$\lambda^{(k)}\nabla g(\mathbf{x}^{(k_1^1)}) = \sum_{j=1}^{M}(\rho_j + \lambda_{1,j}^k - \lambda_{2,j}^k)\log(1+\gamma_j) \tag{6}$$

and the proximal operator in line 7 can be defined as:

$$\mathbf{z}^{k_1^1+1} = \underset{\mathbf{x}\in\mathbb{C}^{N_t\times M}}{\arg\min} \quad \rho_s \sum_{i,j}(1-\beta_{i,j})|x_{i,j}| + \frac{\left\|\mathbf{x}-\mathbf{x}^{k_1^1+1}\right\|_{\mathbf{F}}^2}{2\eta_x^{(k_1^1)}}. \tag{7a}$$

whose solution is given by:

$$z_{i,j}{}^{(k_1^1+1)} = \mathcal{S}_\kappa\left(x_{i,j}{}^{(k_1^1+1)}\right) \tag{8a}$$

$$= \begin{cases} x_{i,j}{}^{(k_1^1+1)} - \kappa, & x_{i,j}{}^{(k_1^1+1)} \geq \kappa, \\ 0, & |x_{i,j}{}^{(k_1^1+1)}| < \kappa \\ x_{i,j}{}^{(k_1^1+1)} + \kappa, & x_{i,j}{}^{(k_1^1+1)} \leq -\kappa, \end{cases}, \tag{8b}$$

where $[\cdot]_{i,j}$ stands for the i,j-th matrix element and $\mathcal{S}_\kappa(\cdot)$ is the (elementwise) *soft thresholding* operation with threshold $\kappa = \eta_x^{(k_1^1)} \cdot \rho_s \cdot (1-\beta_{i,j})$.

Algorithm 1 Proximal-Gradient Dual Ascent (PGDA) Selective Beamforming

1: **Initialization:**
2: Initialize $\mathbf{x}^{(0)}$, $\lambda^{(0)}$, $\mu^{(0)}$, and tol.
3: **for** $k = 0, 1, 2, \ldots$ until convergence **do**
4: $\mathbf{x}$-update using gradient ascent:
5: **while** $L(\mathbf{z}^{(k_1^1)}, \lambda, \mu) < L(\mathbf{z}^{(k_1^1-1)}, \lambda, \mu) + \langle \nabla L(\mathbf{z}^{(k_1^1-1)}, \lambda, \mu), \mathbf{z}^{(k_1^1)} - \mathbf{x}^{(k_1^1-1)} \rangle - \frac{1}{2\eta_x}\|\mathbf{z}^{(k_1^1)} - \mathbf{x}^{(k_1^1-1)}\|_2^2$ **do**
6: $\mathbf{x}^{(k_1^1+1)} = \mathbf{x}^{(k_1^1)} + \eta_x \left(\nabla f(\mathbf{x}^{(k_1^1)}) + \lambda^{(k)} \nabla g(\mathbf{x}^{(k_1^1)}) - 2\mu^{(k)}\mathbf{x}^{(k_1^1)}\right)$
7: $\mathbf{z}^{k_1^1+1} = \text{prox}_{\eta_x^{k_1^1} \cdot \rho_s \cdot \sum_{i,j}(1-\beta_{i,j})|w_{i,j}|}\left(\mathbf{x}^{(k_1^1+1)}\right)$
8: $\eta_x^{(k_1^1+1)} = \alpha * \eta_x^{(k_1^1)}$
9: **end while**
10: $\mathbf{x}^{(k+1)} = \mathbf{z}^{(k_1^1+1)}$
11: λ- and μ-update:
12: $\lambda_{1,j}^{(k+1)} = \max(0, \lambda_{1,j}^{(k)} - \alpha(R_{\min_j} - g(\mathbf{x}^{(k+1)})))$
13: $\lambda_{2,j}^{(k+1)} = \max(0, \lambda_{2,j}^{(k)} - \alpha(g(\mathbf{x}^{(k+1)}))$
14: $\mu^{(k+1)} = \max(0, \mu^{(k)} - \alpha(\text{trace}(\mathbf{x}^{(k+1)}\mathbf{x}^{(k+1)H}) - P))$
15: **if** $\|\mathbf{x}^{(k+1)} - \mathbf{x}^{(k)}\|_2 <$ tol **then**
16: **break**
17: **end if**
18: **end for**

V. Experimental Results

The goal of the simulation is to understand how different bandwidth allocations and beamforming strategies affect the overall performance of the communication system. The Ultra Massive MIMO communication model simulates a multi-user communication scenario with a large number of antennas and users. The system operates over a 28 GHz 5G mmWave band, with a total available bandwidth of 3 GHz. Specifically, the system considers 64 transmit antennas ($N_t = 64$) and 4 single-antenna users ($N_r = 4$). The number of communication users is set to 4 ($M = 4$), and the simulation transmits 1000 symbols ($Ns = 1000$) to each user.

The communication channel is modeled as a Rayleigh fading channel with elements drawn from a complex Gaussian distribution.

The simulation runs multiple iterations (10 runs) to compute various performance metrics. These include spectral efficiency (SE), data rates (Ri) and power metrics (PW). The initial beamforming weights w are generated as complex Gaussian random values. The minimum data rate constraints are set to ensure each user receives at least 100 Mbps within their allocated bandwidth. The total transmit power is set to $Pt = 2kW$.

Initial values for λ_1 and λ_2 are randomly chosen as 0.04 and 0.06, respectively. μ is also initiated at 0.05. The step sizes (η_x) and (α) are set to 0.025 and the maximum number of iterations per simulation run is set to 3000. the tolerance for convergence is 10^{-12}.

The simulated reliability matrix is shown in Figure 1. Each row has a reliability value between 0 and 1 reflecting the reliability of the corresponding antenna element.

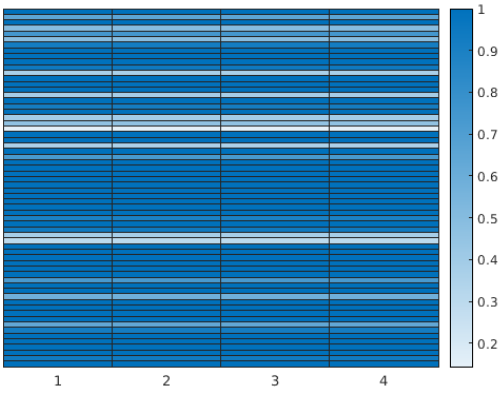

Fig. 1: Heatmap of antenna reliability matrix

We use the dual proximal-gradient algorithm (1) to solve problem (5) for different values of sparisty embedding weight γ. The spectral efficiency over iterations for different levels of sparsity is shown in Figure 2 below. The algorithm achieves higher spectral efficiency levels with denser beamforming (i.e., low γ values) but this comes at the expense of reliability as will be explained next.

γ	Avg. SE (bps/Hz)	Avg. Ri (Gbps)	RL (%)	BMD (%)	PW (kW)
0	2.3238	1.7429	0.0000	100.0000 ± 0.0000	1.9630 ± 0.2013
3.3340	2.2572	1.6929	0.0000	92.5781 ± 0.5524	1.7945 ± 0.3311
33.3400	1.8978	1.4234	1.4533	72.0312 ± 0.5881	1.8413 ± 0.2281
166.7000	1.8239	1.3679	67.6410	66.2500 ± 0.2731	1.8594 ± 0.2476
333.4000	1.7821	1.3366	92.9565	64.4531 ± 0.1841	1.8929 ± 0.2935

TABLE I: Summary of System Performance Metrics for Different γ Values

The table summarizes system performance across various values of the sparsity promotion weight, γ, highlighting its impact on spectral efficiency (SE), communication rate (R_i), antenna reliability (RL), beamforming matrix density (BMD), and power consumption (PW).

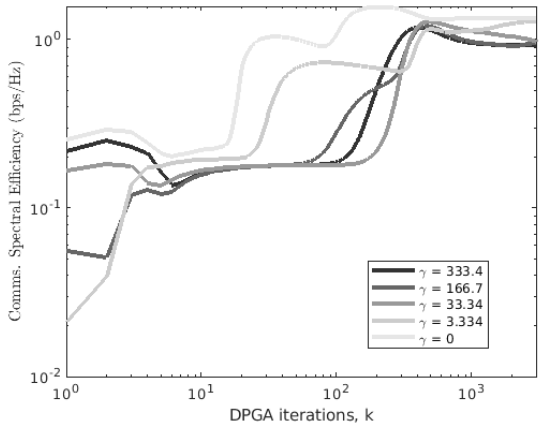

Fig. 2: Spectral Efficiency vs DPGA iterations for different sparsity promotion weights (γ).

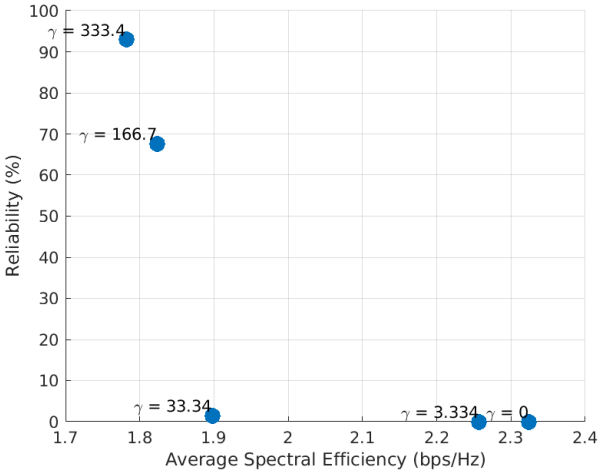

Fig. 3: Reliability vs Spectral Efficiency trade-off.

At $\gamma = 0$, with no sparsity promotion, the system achieves peak performance with an SE of 2.3238 bps/Hz and a communication rate of 1.7429 Gbps. The beamforming matrix is fully populated (BMD = 100%), indicating no sparsity, which results in maximum power consumption (1.9630 kW) and no redundancy in antenna usage (RL = 0%).

As γ increases to 3.3340, SE and R_i decrease slightly to 2.2572 bps/Hz and 1.6929 Gbps, respectively. The BMD drops to 92.5781%, introducing some sparsity while reducing power consumption to 1.7945 kW. Despite this shift, antenna reliability remains at zero, indicating no redundancy has yet been introduced.

At $\gamma = 33.3400$, the system shows more pronounced sparsity effects. SE and R_i decline further to 1.8978 bps/Hz and 1.4234 Gbps. The BMD drops to 72.0312%, while power consumption increases slightly to 1.8413 kW. Antenna reliability rises to 1.4533%, suggesting the system is beginning to prioritize redundancy in certain antenna elements.

With $\gamma = 166.7000$, SE and R_i continue to decline to 1.8239 bps/Hz and 1.3679 Gbps, respectively. The BMD reduces significantly to 66.2500%, while power consumption rises slightly to 1.8594 kW. Notably, RL increases sharply to 67.6410%, indicating substantial redundancy in the beamforming structure. This reflects a system trading efficiency and throughput for enhanced robustness.

At the highest sparsity setting ($\gamma = 333.4000$), SE and R_i reach their lowest values at 1.7821 bps/Hz and 1.3366 Gbps. The BMD falls to 64.4531%, reflecting maximum sparsity. Power consumption marginally rises to 1.8929 kW, while RL peaks at 92.9565%, emphasizing strong redundancy to maximize reliability.

Overall, the results reveal a clear trade-off: increasing γ reduces SE and communication rates while promoting sparsity and enhancing system reliability. This behavior highlights the system's ability to balance efficiency, power savings, and robustness depending on the desired performance objective.

Figure 3 depicts the trade-off between reliability and spectral efficiency for different sparsity levels.

Figure 4 and **??** respectively show how power and average rate vary as a function of γ.

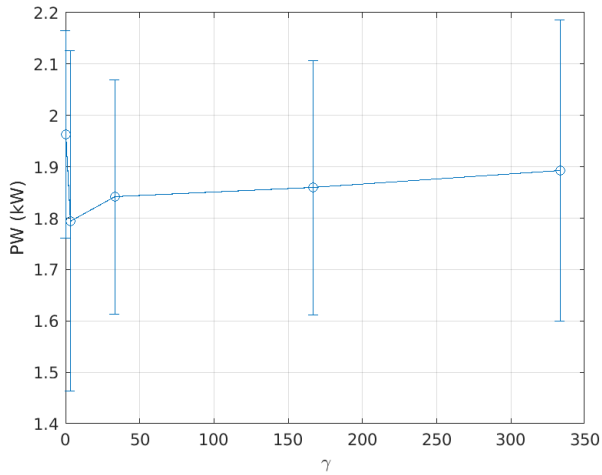

Fig. 4: Power vs sparsity weight.

Figure 5 and Figure 6 below show how sparsity structure is being promoted in going from $\gamma = 0$ (100%-dense beamforming) to $\gamma = 333.4$ (36%-sparse beamforming)).

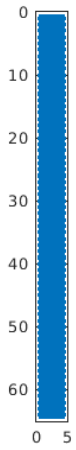

Fig. 5: Beamforming sparsity pattern with γ = 0

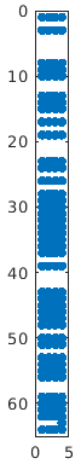

Fig. 6: Beamforming sparsity pattern with $\gamma = 333.34$

Overall, as γ increases, there is a clear trade-off between spectral efficiency, communication rate, and power consumption on one hand, and beamforming matrix sparsity and antenna reliability on the other. The system adjusts its parameters to promote sparsity and reliability, which leads to reduced performance in terms of SE and Ri but increases fault tolerance and potentially extends the operational life of the system by lowering the active usage of all antennas simultaneously. This balance is crucial for designing systems that need to operate efficiently under various constraints and reliability requirements.

VI. CONCLUSION

In this paper, we addressed the optimization challenges inherent in Ultra-Massive MIMO communication systems, particularly focusing on array selection and beamforming under diverse and dynamic operational conditions. By incorporating antenna health information into the optimization process, our novel array selection criterion distinguishes itself from traditional methods, ensuring more robust and reliable system performance. Utilizing gradient dual ascent and dual proximal-gradient ascent methodologies, we effectively tackled the constrained non-convex and non-smooth nature of sparse array selection problems.

Our approach's central feature—implementing proportional fairness among communication users—aligns with system resource limitations while guaranteeing minimum rate requirements for all users. This ensures not only improved system efficiency and responsiveness but also equitable distribution of resources. Extensive simulations validated the proposed solutions, demonstrating their effectiveness in optimizing Ultra-Massive MIMO system performance and their applicability in complex communication scenarios.

The results from our simulations revealed key trade-offs influenced by the sparsity promotion weight (γ). As γ increased, we observed a decrease in spectral efficiency (SE) and communication rate (Ri), which was accompanied by a reduction in the beamforming matrix density (BMD) and a marginal variation in power consumption (PW). However, these changes also led to a significant increase in antenna reliability (RL), highlighting the system's ability to enhance robustness through redundancy. These trade-offs underscore the critical balance between maintaining high performance and ensuring system reliability, which is pivotal for the practical deployment of Ultra-Massive MIMO systems.

Our findings provide new insights and innovative solutions for array selection and beamforming optimization. The incorporation of antenna health into the selection process and the adoption of fairness-driven resource allocation contribute to more resilient and efficient communication networks. This work not only enhances current methodologies but also sets a foundation for future research aimed at further optimizing and understanding the complexities of Ultra-Massive MIMO systems.

The choice of 64 antenna elements is justified as it is a feasible number for computation on a desktop computer. Future work will involve applying this model to scenarios with more than 64 antenna elements to explore further improvements in performance and efficiency. This expansion will help in understanding the scalability and limitations of DPGA in more complex and demanding environments.

APPENDIX

A. Gradient of communication term

Let us use the gradient ascent for the $\mathbf{x}$-update. To find the partial derivative of $\sum_{m=1}^{M} \log(1+\gamma_m)$ with respect to $w_{i,k}$, we will use the chain rule. Given that γ_m has a specific functional form in terms of $w_{i,k}$, we can express the derivative as:

$$\frac{\partial \sum_{m=1}^{M} \log(1+\gamma_m)}{\partial w_{i,k}} = \sum_{m=1}^{M} \frac{1}{1+\gamma_m} \frac{\partial \gamma_m}{\partial w_{i,k}} \tag{9}$$

where

$$\frac{\partial \gamma_m}{\partial w_{i,k}} = \begin{cases} \frac{\mathbf{h}_m \mathbf{h}_m^H \mathbf{w}_m + \mathbf{h}_m \mathbf{h}_m^H \mathbf{w}_m^*}{\sum_{j \neq m} |\mathbf{h}_m^H \mathbf{w}_j|^2 + \sigma_c^2} & \text{if } i = m \\ |\mathbf{h}_m^H \mathbf{w}_m|^2 \frac{\mathbf{h}_m \mathbf{h}_m^H \mathbf{w}_i + \mathbf{h}_m \mathbf{h}_m^H \mathbf{w}_i^*}{(\sum_{j \neq i} \left|\mathbf{h}_i^H \mathbf{w}_j\right|^2 + \sigma_c^2)^2} & \text{if } i \neq m \end{cases} \tag{10}$$

or

$$\frac{\partial \gamma_m}{\partial w_{i,k}} = \begin{cases} \frac{\mathbf{h}_m \mathbf{h}_m^H \mathbf{w}_m + \mathbf{h}_m \mathbf{h}_m^H \mathbf{w}_m^*}{\sum_{j \neq m} |\mathbf{h}_m^H \mathbf{w}_j|^2 + \sigma_c^2} & \text{if } i = m \\ \gamma_m \frac{\mathbf{h}_m \mathbf{h}_m^H \mathbf{w}_i + \mathbf{h}_m \mathbf{h}_m^H \mathbf{w}_i^*}{\sum_{j \neq i} \left|\mathbf{h}_i^H \mathbf{w}_j\right|^2 + \sigma_c^2} & \text{if } i \neq m \end{cases} \tag{11}$$